CONF-8610159--3

International Symposium on the Physics and Chemistry of Small Clusters, Richmond, VA, October 28-November 1, 1986

METASTABLE DECAY OF PHOTOIONIZED NIOBIUM CLUSTERS: EVAPORATION VS. FISSION FRAGMENTATION

S. K. Cole, K. Liu, and S. J. Riley

Chemistry Division
Argonne National Laboratory
Argonne, IL 60439 USA

CONF-8610159--3

DE87 004314

ABSTRACT

The metastable decay of photoionized niobium clusters (Nb_n^+) has been observed in a newly constructed cluster beam machine. The decay manifests itself in the time-of-flight (TOF) mass spectrum as an asymmetric broadening of daughter ion peaks. Pulsed ion extraction has been used to measure the decay rate constants and to establish the mechanism of the fragmentation, evaporation and/or fission of the photoionized clusters. It is found that within the experimental time window evaporation dominates for the smaller clusters ($n<15$), whereas fission fragmentation becomes facile for $15<n<30$. The decay rate constants obtained all fall within the range $0.5\text{-}2.0 \times 10^6$ sec^{-1}. The average kinetic energy release is also determined and is found to be on the order of 5 meV.

I. INTRODUCTION

Fragmentation of atomic cluster ions has been studied in a number of recent experiments.[1-7] The observed fragmentation patterns appear to fall into distinct categories depending on the types of clusters. In general, metal clusters tend to lose one atom at a time (evaporation), whereas semiconductor clusters exhibit both evaporation and fission fragmentation (cleavage of a large cluster). From the pieces of information available, it seems that fragmentation patterns generally reflect the relative stability of the fragments. However, this conjecture still does not explain why the fragmentation pattern should be different for metal and semiconductor clusters. In this study, we report the first observation of fission fragmentation for a transition metal cluster. It is found that there is a critical cluster size above which fission fragmentation becomes facile, analogous to the nuclear fission process.

II. EXPERIMENTAL

The apparatus consists of an ion time-of-flight (TOF) mass spectrometer and an electron TOF spectrometer coupled with a laser vaporization source for generation of the metal clusters. The second harmonic

of a 20 Hz Nd:YAG laser is weakly focused onto a niobium rod resulting in vaporization of the metal. A pulsed flow of He cools the plasma and stimulates cluster growth. For the study of neutral clusters various excimer lasers are used for ionization prior to extraction into the TOF apparatus. TOF mass spectra have been obtained at four photon energies: 6.4 eV (ArF excimer laser), 5.0 eV (KrF excimer laser), 4.0 eV (XeCl excimer laser), and 3.5 eV (XeF excimer laser).

III. PHOTOFRAGMENTATION PATHWAY

Figure 1 shows a portion of the TOF mass spectrum of Nb clusters for two different photoionizing lasers. In the case of 5 eV photons (KrF excimer laser), the peaks show a distinct asymmetric broadening, while 6.4 eV photons (ArF laser) produce much less broadening. Also, the broadening is specific to cluster size, being very pronounced for some clusters (such as Nb_7^+) and much less so for others (such as the fragments Nb_6^+ and Nb_8^+). This broadening persists even for KrF laser fluences as low as 20 $\mu J/cm^2$. TOF mass spectra have also been obtained using a XeCl excimer laser and a XeF laser for ionization of the neutral clusters. These spectra are very similar to the KrF spectrum.

Metastable decay of molecular ions in a TOF mass spectrometer is a well understood phenomenon. The signature of such a process, asymmetric broadening of daughter ion peaks, is a consequence of parent ion fragmentation on a time-scale comparable to the ion extraction time. If the dissociation takes place after the parent ion has experienced significant acceleration, but before the acceleration is complete, the daughter ion time of flight will be between that of the parent ion and an unfragmented daughter ion. The width and shape of the asymmetric broadening will depend upon the time-of-flight parameters, i.e., voltages and distances, and the nature of the fragmentation. In a typical experiment of this type, all parameters are known except the parent ion dissociation rate for a particular daughter ion and the kinetic energy released in the dissociation. These two unknowns can be determined from the TOF spectrum. However, in the case of a distribution of cluster sizes, the parent ion is also unknown, thereby complicating the analysis. To sort out what processes are occurring, a delayed ion extraction technique has been used in this study to determine the dissociation rates for niobium clusters in the size range 5 to 30.

Though the asymmetric broadening of the ion peaks in the KrF spectrum might be due to ion metastable decay, other possible mechanisms must be considered and tested. For example, a delayed ionization process such as dissociative ionization, field ionization, or ion pair formation followed by autodetachment will also result in asymmetric broadening of the TOF peaks. These processes will also broaden the electron TOF spectrum. The observed electron TOF spectrum shows but a single sharp peak (FWHM < 30 ns), which rules out any delayed ionization proc-

ess. Ion-molecule reactions during ion extraction might also result in a metastable peak shape. To test this possibility the delayed ion extraction technique was used. If an ion-molecule reaction is occurring the peak shape will be independent of the extraction time. As can be seen in Fig. 2 this is not the case. With increasing delay between the laser pulse and the ion extraction pulse the ion peaks become sharper, indicating that an ion-molecule reaction is not responsible for the observed peak shapes.

More importantly, since the delayed ion extraction technique is, in essence, a mass spectrometric version of the pump-and-probe method, it should provide a direct measurement of the absolute decay rate constant. This may be seen by considering a single exponential decay of a parent ion cluster of size m to a daughter ion i.

$$Nb_m^+ \rightarrow Ni_i^+ + Nb_{m-i} \cdot \qquad (1)$$

The number of daughter ions formed per unit time at time τ can be expressed as:

$$dn_i/d\tau = k_{m\rightarrow i}\, n_m^0 \exp(-k_m\tau) \qquad (2)$$

where n_m^0 is the initial parent ion number density, k_m is the total decay rate constant of the parent ion, and τ is the time after photoexcitation.

Since the actual data is displayed in the TOF time domain, one has to consider the mapping of the formation times τ of a daughter ion in the ion source into the arrival times t at the detector. For each parent and daughter mass in a given electric field there is a unique transformation from the TOF time domain into the real decay time domain. Furthermore, it is found that under space focusing conditions the transformation is approximately a linear function, i.e., $\tau = \alpha t$. Therefore the rate equation becomes

$$dn_i/dt = k'_{m\rightarrow i}\, n_m^0 \exp(-k'_m t) \qquad (3)$$

where $k'_m = \alpha k_m$ is the "apparent" decay constant in the TOF time domain and α is the transformation coefficient. Thus, the signal in the TOF spectrum should also behave as an exponential decay. One can readily extend the above analysis to the case of several parent ions or isomers.

Figure 3 gives some indication of the validity of this approximation, in which the Nb_7^+ daughter ion peak is simulated by a double exponential decay of metastable parent ions. At least two components are necessary to fit the peak. The data fitting is conducted in two steps. First, the "slow" component (tailing to long time of flight) is fit by a single exponential. The "fast" component is then fit by a single exponential after subtracting the TOF signal form the "slow" component fit. The ratio of the preexponential factor divided by the apparent rate con-

stant to the total peak intensity then gives the fraction of ions resulting from each metastable decay component.

In the case of pulsed ion extraction with a time delay ΔT between the photon pulse and the extraction pulse, Eq. (3) becomes:

$$dn_i/dt = [k'_{m\rightarrow i}\, n_m^0 \exp(-k_m \Delta T)] \exp(-k'_m t) \qquad (4)$$

where t is still in the TOF time domain but starts from the onset of the delayed extraction pulse. The idea of the delayed extraction technique is to follow the time evolution of the amount of metastable decay with the variable time delay ΔT as illustrated in Fig. 2. Quantitatively, it can readily be shown from Eq. (4) that the fraction of the total signal in the metastable tail should be proportional to $\exp(-k_m \Delta T)$. Thus, the slope of a plot of ln(fraction) vs. ΔT yields the decay rate constants k_m directly. Once the rate constants k_m and k'_m are known for a given daughter ion, the transformation coefficient α, and hence the parent ion mass, can be determined.

Table I summarizes the results for Nb_i^+ daughter ions $5 \leq i \leq 15$. Note that the decay rate constants are nearly all identical. The evaporation component appears "fast" simply as a result of the time domain transformation (α is large). The identification of the parent ion for the evaporation component is in fact simplified by the transformation, because α is a rapidly varying function of the parent ion and daughter ion masses in this mass range. On the other hand, as the ratio of the parent to daughter ion masses increases, α becomes less sensitive to the exact parent mass. Therefore, there is a range of parent ion masses for the fission fragmentation.

It is worthwhile to point out several interesting findings from these experiments. (1) For cluster ions Nb_n^+ in the size range n=7 to 15, all TOF peaks exhibit two distinct components to their asymmetric broadening. As shown in Table I, one results from the fission fragmentation of the larger cluster ions Nb_{15}^+ to Nb_{30}^+, and the other from evaporation of monomers and dimers from clusters having one or two more niobium atoms than the observed daughters. However, the daughter ions 5 and 6 result only from evaporation pathways. (2) For decay processes occurring within the experimental time window (0.1 to 60 μs), evaporative fragmentation dominates for the smaller parent clusters ($6 \leq n \leq 15$), while fission fragmentation becomes facile for $15 < n < 30$. (3) The rate constants for fragmentation of all parent clusters except Nb_7^+ are within the range 0.5 to 2×10^6 sec^{-1}. The Nb_7^+ cluster is surprisingly stable and undergoes no fragmentation once it is formed. This stability is also evidenced by the high intensity daughter ion signal for Nb_7^+ seen in Fig. 1. Other evidence for a stable Nb_7^+ ion is seen in the spectrum of cluster ions coming directly from the source, where once again Nb_7^+ is the most prominent species. In fact, there are other

Table 1. Fragmentation Decay Rates for $Nb_m^+ \rightarrow N_i^+ + Nb_{m-i}$

	EVAPORATION ("fast")			FISSION ("slow")			
i	$k_{evap.}$ (10^6 s^{-1})	Parent Ion (m)	Fraction[a]	$k_{fiss.}$ (10^6 s^{-1})	Parent Ion (m)	Fraction[a]	Total Fraction[b]
5	0.90	6	0.20	-	-	-	0.20
6	1.41	8	0.27	-	-	-	0.27
7	2.04	9	0.29	0.85	17-30	0.59	0.88
8	1.82	10	0.24	0.70	14-17	0.32	0.56
9	1.81	10,11	0.35	0.61	16-20	0.67	1.02
10	0.82	11	0.26	0.56	16-19	0.33	0.59
11	1.06	12	0.24	0.78	21.24	0.39	0.63
12	0.74	13	0.26	0.64	20.24	0.39	0.65
13	0.94	14	0.22	0.75	25-30	0.50	0.72
14	0.69	15	0.16	0.62	24-27	0.47	0.63
15	0.64	16	0.15	0.61	23-28	0.51	0.66

[a]Refers to the ratio of the integrated intensity of the particular component relative to the total integrated intensity of the ion peak.
[b]Refers to the fraction of the total integrated peak intensity due to fragmentation (evaporation and fission).

similarities between the spectra of ions from the source and from metastable decay. (4) The average kinetic energy imparted to the daughter ions has been measured and found to be on the order of 5 meV. This low energy, together with the observation that fragmentation tends to lead to the more stable ionic clusters, suggest that the fragmentation processes are statistical in nature and have no substantial reverse activation barriers.

IV. PHOTOEXCITATION PATHWAY

To better understand the fragmentation pathways observed here, a series of experiments has been conducted to elucidate the photoexcitation pathway and the energetics involved. The dependence of the ion signal on laser fluence shows a slope of 1.2 for the KrF laser excitation and 0.9 for the 6.4 eV ArF excitation. In the size range n=5 to 30, niobium clusters have ionization potentials ranging from 4.5 to 5.5 eV.[8] Thus it appears KrF laser ionization is a two-photon process. Interestingly, preliminary photoelectron energy measurements indicate that the average kinetic energies of photoelectrons from KrF and ArF laser ionization are not very different, being 0.8 eV for KrF and 1.3 eV for ArF. An additional observation is that when the KrF laser is fired at the cluster ions coming from the source, no asymmetric broadening appears.

This complex series of observations points to the following picture of the photophysical and photochemical processes in Nb clusters. When parent neutral clusters absorb one KrF photon, even if the cluster ionization potential is lower than 5 eV, only a small fraction of them ionize. This is consistent with the TOF spectrum in which the parent ion signals are much smaller than the daughter ion signals. The more probable ionization pathway is the absorption of an additional photon followed by ionization and fragmentation into daughter ions. This tentative scenario may have important implications for the study of transition metal clusters because it requires the existence of some isolated excited states which have little coupling with the rest of the "vibronic soup" that is thought to characterize transition metal clusters. A direct experimental verification of this photoexcitation pathway is currently under way.

Acknowledgments: KL would like to thank Dr. E. K. Parks for his help in construction of the apparatus.

REFERENCES

1 P. J. Brucat, L.-S. Zheng, C. L. Pettiette, S. Yang, and R. E. Smalley, J. Chem. Phys. **84**, 3078 (1986).

2 J. R. Heath, Y. Liu, S. C. O'Brien, Q.-L. Zhang, R. F. Curl, F. K. Tittle, and R. E. Smalley, J. Chem. Phys. **83**, 5520 (1985).

3 L. A. Bloomfield, R. R. Freeman, and W. L. Brown, Phys. Rev. Lett. 54, 2246 (1985).

4 W. Begemann, K. H. Meiwes-Broer, and H. O. Lutz, Phys. Rev. Lett. 56, 2248 (1986).

5 M. E. Geusic, T. J. McIlrath, M. F. Jarrold, L. A. Bloomfield, R. R. Freeman, and W. L. Brown, J. Chem. Phys. **84**, 2421 (1986).

6 C. Brechignac, Ph. Cahuzac, and J. Ph. Roux, Chem. Phys. Lett. 127, 445 (1986).

7 C. Brechignac and Ph. Cahuzac, Chem. Phys. Lett. **112**, 20 (1984).

8 R. L. Whetten, M. R. Zakin, D. M. Cox, D. J. Trevor, and A. Kaldor, J. Chem. Phys. 85, 1697 (1986).

This work is supported by the U. S. Department of Energy under contract W-31-109-Eng-38.

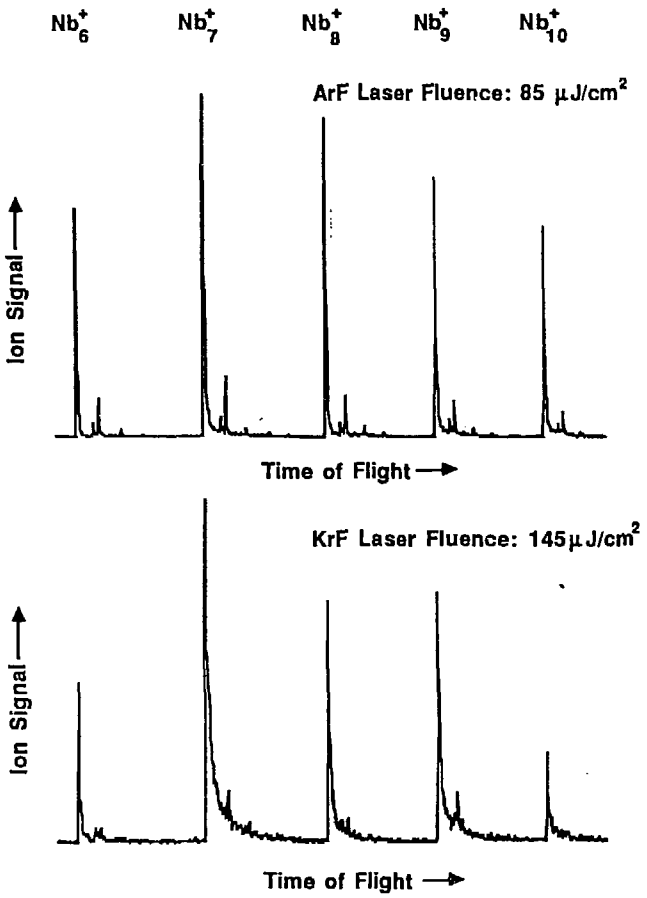
Nb_6^+
Nb_7^+
Nb_8^+
Nb_9^+
Nb_{10}^+
ArF Laser Fluence: 85 μJ/cm²
Ion Signal
Time of Flight
KrF Laser Fluence: 145μJ/cm²
Ion Signal
Time of Flight

Fig. 1

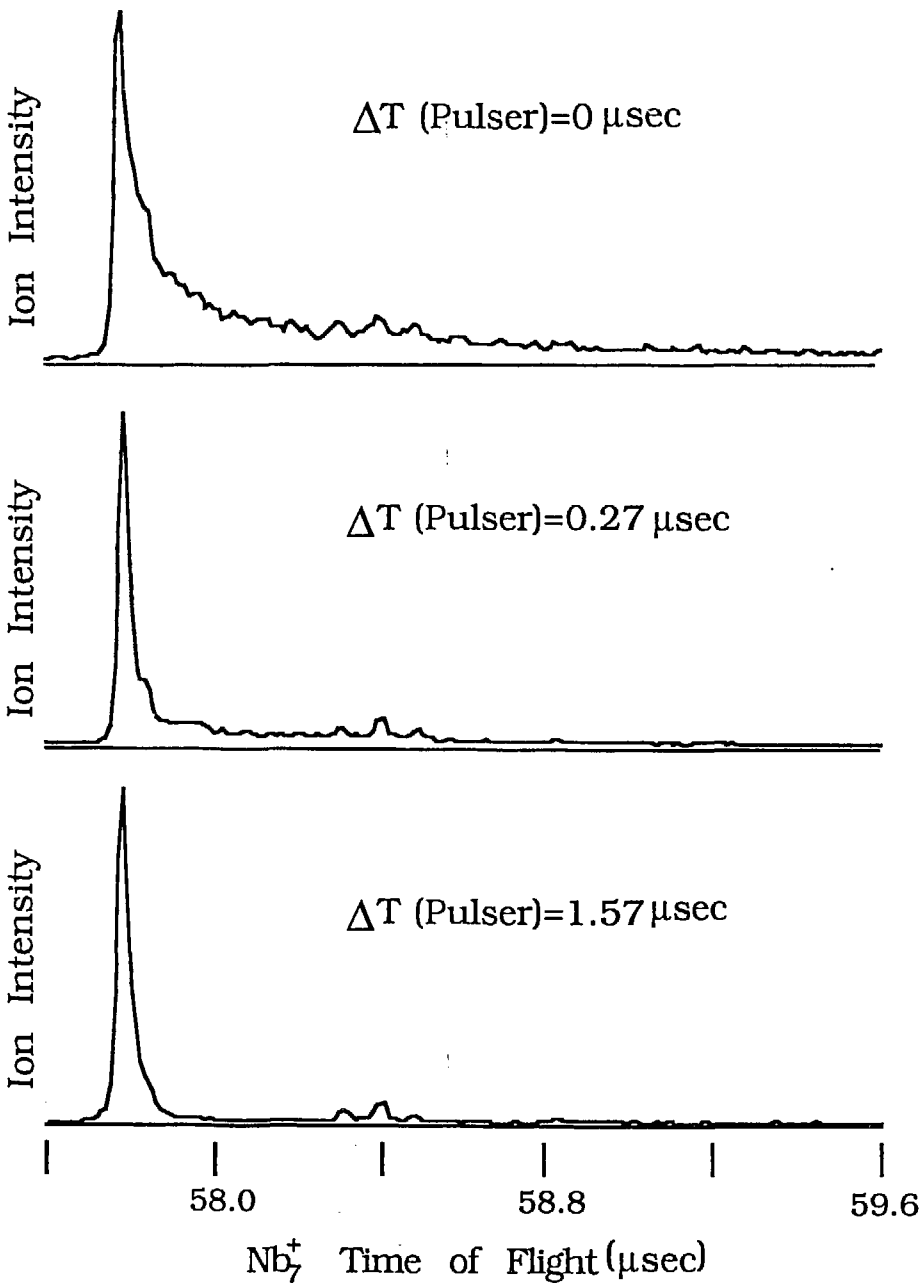
Ion Intensity
ΔT (Pulser)=0 μsec
Ion Intensity
ΔT (Pulser)=0.27 μsec
Ion Intensity
ΔT (Pulser)=1.57 μsec
58.0
58.8
59.6
Nb_7^+ Time of Flight (μsec)

Fig. 2

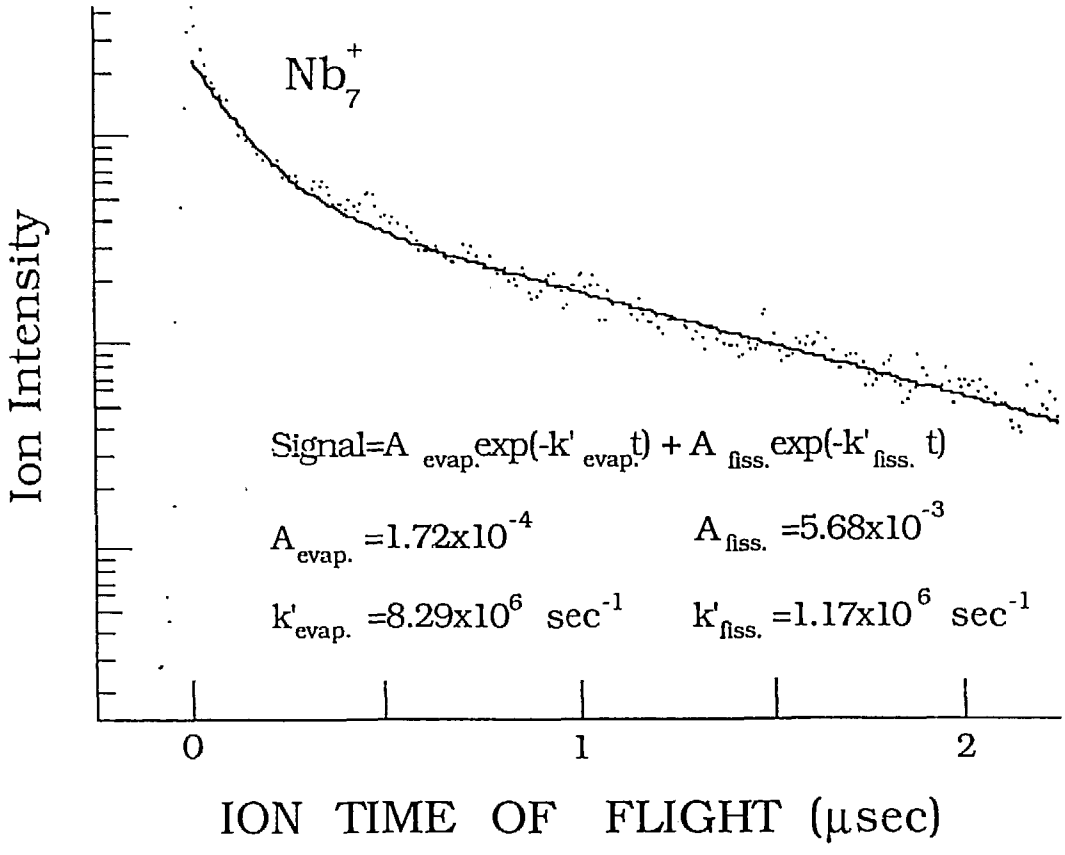

Fig. 3.